The physical properties of white dwarf-main sequence binaries from SDSS

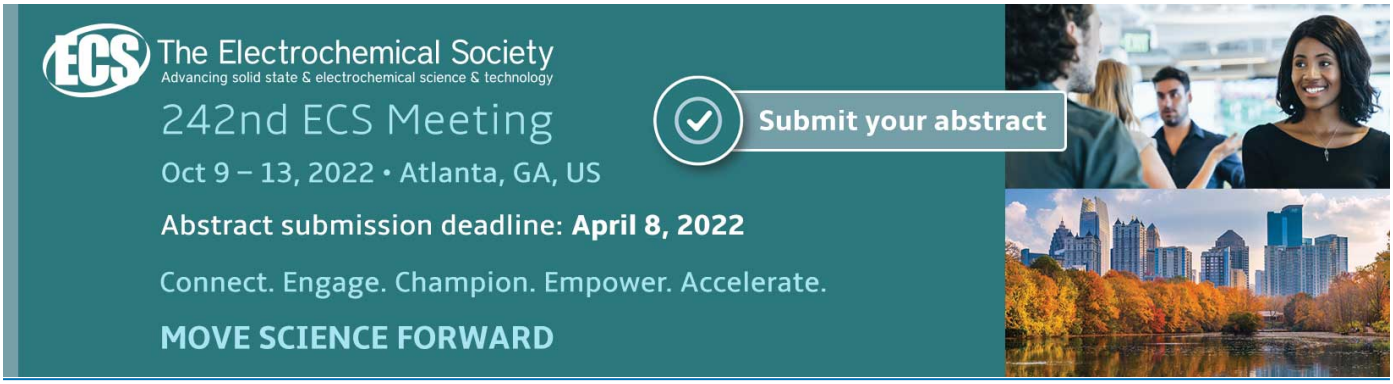

Journal of Physics: Conference Series **172** (2009) 012025 doi:10.1088/1742-6596/172/1/012025

The physical properties of white dwarf-main sequence binaries from SDSS

A Rebassa-Mansergas[1], B T Gänsicke[1] and D Koester[2]

[1]University of Warwick, Coventry CV4 7AL, UK

[2] Institut für Theoretische Physik und Astrophysik, University of Kiel, 24098 Kiel, Germany

E-mail: A.Rebassa-Mansergas@warwick.ac.uk

Abstract. We present a catalogue of 1596 white dwarf-main sequence binaries (WDMS) from the spectroscopic Sloan Digital Sky Survey Data Release 6 (SDSS DR6). We select WDMS binary candidates from template fitting all 1.27 million DR6 spectra, using combined constraints in both χ^2 and signal-to-noise ratio (S/N). In addition, we use Galaxy Evolution Explorer (GALEX) and UKIRT Infrared Sky Survey (UKIDSS) magnitudes to search for objects in which one of the two components dominates the SDSS spectrum. We use a decomposition/fitting technique to measure the effective temperatures, surface gravities, masses and distances to the white dwarfs, as well as the spectral types and distances to the companions in our catalogue.

1. Introduction

Binaries containing a white dwarf primary plus a main sequence companion were initially main sequence binaries in which the more massive star evolved through the giant phase and became a white dwarf. In the majority of cases the initial separation of the main sequence binary is wide enough to allow the evolution of both stars as if they were single. Nevertheless, a small fraction are believed to undergo mass transfer interactions (Webbink 1984, de Kool 1992, Willems & Kolb 2004). The more massive star will engulf its companion while evolving into a red giant, and the system enters a common envelope (CE, Iben & Livio 1993, Webbink 2007). Friction inside this envelope causes a rapid decrease of the binary separation. Henceforth orbital energy and angular momentum are extracted from the binary orbit and lead to the ejection of the envelope, exposing a post-common-envelope binary (PCEB). After the ejection of the envelope, close WDMS binaries evolve to shorter orbital periods through angular momentum loss via magnetic braking.

Population synthesis models have been developed for the understanding of both CE evolution and magnetic braking (e.g. Politano & Weiler 2007, Davis et al. 2008). Nonetheless the results provided by these works clearly lack observational constraints, and the advance in our understanding of CE evolution and magnetic braking is consequently most likely to arise from the analysis of PCEBs that are both numerous and well-understood in terms of their stellar components. It becomes then necessary to dispose of a large sample of observable WDMS binaries to constrain the evolution of close binaries. The SDSS (York et al. 2000, Stoughton et al. 2002, Adelman-McCarthy et al. 2008) has offered the opportunity of increasing the number of WDMS binaries available for follow-up studies. Here we make use of the SDSS spectroscopic DR6 to create a catalogue of 1596 WDMS binaries and candidates. In a parallel work, within

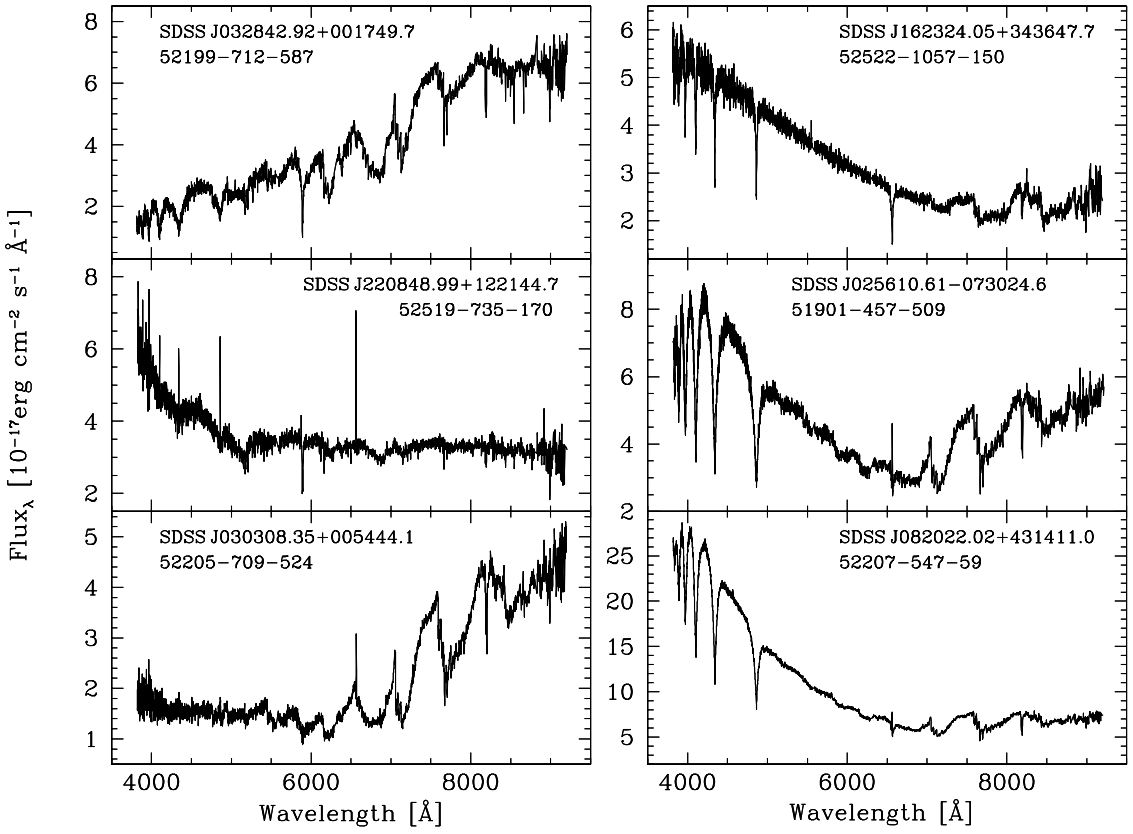

Figure 1. Six examples of previously known WDMS binaries used in this work as WDMS binary templates. SDSS names and MJD-PLT-FIB identifiers are indicated for each of them.

SEGUE we are also running a dedicated program to identify WDMS binaries containing cold white dwarfs (Schreiber et al. 2007). This sample of more than 1500 WDMS binaries is an excellent database for future follow-up observational studies of WDMS binaries (Schreiber et al. 2008, Rebassa-Mansergas et al. 2008, Pyrzas et al. 2008, Nebot Gomez-Moran et al. 2008).

2. Identification of WDMS binaries in SDSS

2.1. Computational method

We have developed a procedure based on χ^2 template fitting in order to automatically identify WDMS binary candidates from the SDSS DR6 spectroscopic data base. Our initial template set consisted of several dozen SDSS spectra of confirmed WDMS binaries from Eisenstein et al. (2006) and Silvestri et al. (2007). These spectra were chosen to sample a wide variety of white dwarfs and companion stars, and to be of high S/N. A set of representative templates is shown in Fig. 1. In addition, we compiled a set of 17 single DA white dwarf template spectra from Eisenstein et al. (2006)'s list, covering the entire observed range of $T_{\rm eff}$ and $\log g$, as well as the M0-M9 Bochanski et al. (2007) M-dwarf templates.

Each of these WDMS binary, white dwarf, and M-dwarf templates were then fitted to the full 1.27 million spectra in DR6. In this process, the template spectrum was normalised to the SDSS spectrum under scrutiny, and a reduced χ^2 was calculated using the errors of the two spectra added in quadrature. In practice, our fitting procedure produced for each of the WDMS

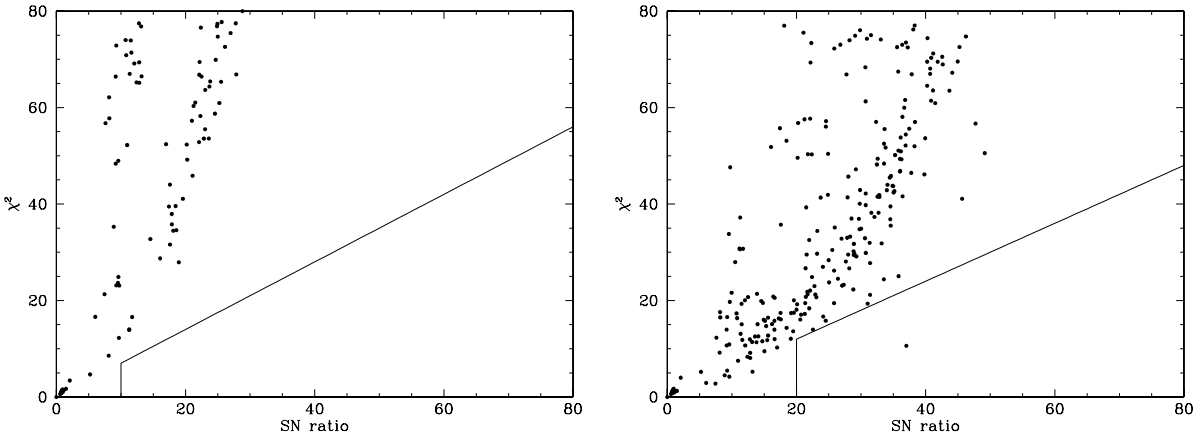

Figure 2. χ^2 − S/N plane obtained fitting two of our WDMS binary templates (SDSS J103121.97+202315.1, left and SDSS J204431.44-061440.2, right) to the 640 objects contained in the SDSS spectral plate PLT = 2295. Objects falling in the area defined by $\chi^2_{\rm spec} < a \times {\rm S/N}$ and ${\rm S/N_{spec}} > {\rm S/N_{min}}$ were considered WDMS binary candidates. Left panel: ${\rm S/N_{min}} = 10$ and $\chi^2_{\rm max} = 0.7 \times {\rm S/N}$, no WDMS binary candidate is identified. Right panel: ${\rm S/N_{min}} = 20$ and $\chi^2_{\rm max} = 0.6 \times {\rm S/N}$, one WDMS binary candidate is found.

binary, white dwarf, and M-dwarf templates a list of spectrum identifier (MJD-PLT-FIB), S/N of the spectrum, and χ^2 for all SDSS DR6 spectra. For each of the templates, we plotted χ^2 as a function of S/N, and defined a minimum value of S/N, ${\rm S/N_{min}}$, and a linear relation $\chi^2_{\rm max} = a \times {\rm S/N}$. We considered any spectrum with

$$\chi^2_{\rm spec} < \chi^2_{\rm max} \quad \text{and} \quad {\rm S/N_{spec}} > {\rm S/N_{min}} \tag{1}$$

as a WDMS binary, white dwarf, or M-dwarf (depending on the current template). ${\rm S/N_{min}}$ had to be set to avoid being swamped by spectra that are too noisy for any definite identification, and the S/N-dependent form of $\chi^2_{\rm max}$ accounts for the increase of χ^2 for higher values of S/N. Both constraints were defined individually for each of the templates, as the different spectral shapes resulted in a large spread of χ^2 distributions. The (χ^2, S/N) planes obtained from fitting the spectra of a single spectral plate (640 spectra) are shown for two different WDMS binary templates in Fig. 2.

After a first run through the DR6 spectra, we complemented the template set with the spectra of a number of newly identified WDMS binaries, and re-run the fitting for those new templates again. That process was repeated until no new WDMS binary candidates were found – at which point we had used a total of 163 different WDMS binary template spectra.

2.2. Red and blue excess in SDSS spectra: help from GALEX and UKIDSS

While the template fitting proved to be a robust method to find WDMS binaries in which both stellar components contribute clearly visible amounts of flux, the procedure is prone to misclassify white-dwarf dominated WDMS binaries as single white dwarfs, and M-dwarf dominated WDMS binaries as single M-dwarfs. We therefore decided to probe more specifically for the presence of excess flux at the red (blue) end of the SDSS spectra in objects classified initially as single white dwarfs (M-dwarfs).

For the search of red flux excess in single white dwarf candidates, we fitted synthetic white dwarf spectra computed with the code described by Koester et al. (2005) to the SDSS spectra, and then calculated the reduced χ^2 over the wavelength ranges 4000 − 7000 Å ($\chi^2_{\rm b}$)

and $7000 - 9000$ Å ($\chi^2_{\rm r}$). Objects with $\chi^2_{\rm r}/\chi^2_{\rm b} > 1.5$ were "promoted" from single white dwarf candidates to WDMS binary candidates (see top and middle left panels of Fig. 3).

The search for blue flux excess proceeded in an analogous fashion for the single M-dwarf candidates, only that we used the set of high S/N M-dwarf templates from Rebassa-Mansergas et al. (2007) instead of model spectra, and calculated the reduced χ^2 over the wavelength ranges $4000 - 5000$ Å and $7000 - 9000$ Å. Objects with $\chi^2_{\rm b}/\chi^2_{\rm r} > 1.5$ were "promoted" from single M-dwarf candidates to WDMS binary candidates (see top and middle right panels of Fig. 3). However, in several cases, the detection of blue or red flux excess is rather marginal.

As a final step in our search for WDMS binaries, we have cross-correlated our entire list of WDMS binaries candidates identified above with the GALEX DR4, providing near- and far-ultraviolet magnitudes, and with the DR4 of UKIDSS, providing infrared $yJHK$ magnitudes. We then inspected the observed ultraviolet-optical spectral energy distribution of all secondary star dominated WDMS binary candidates with available GALEX magnitudes, and the optical-infrared spectral energy distribution of all white dwarf dominated WDMS binary candidates with available UKIDSS magnitudes. Objects where a clear ultraviolet or infrared excess was detected were then included in our WDMS binary sample (see bottom panels of Fig. 3).

2.3. SDSS images

As a final check on the nature of the WDMS binary candidates, we inspected their SDSS DR6 images for morphological problems, and found primarily two types of issues.

Occasionally, single white dwarfs (M-dwarfs) may be located close to very bright M-dwarfs (white dwarfs or A-stars), which will cause scattered light to enter the spectroscopic fibre, and result in an (apparent) two-component spectrum. A spectacular example is SDSSJ 073531.86+315015.2 (left panels of Fig. 4), where the SDSS spectrum clearly exhibits an M-dwarf at red wavelengths, and a blue component with strong Balmer lines in the blue – the SDSS image reveals that this is a single M-dwarf at a distance of 12 arcmin of Castor A/B – two $V = 2 - 3$ A-stars. The SDSS magnitudes (black dots) are superimposed to the SDSS spectrum (gray) and are consistent with those of a single red star. In addition, single M-dwarfs are also likely to be found superimposed with single early-type stars in the same image. An example is SDSSJ 005827.24+005642.6 (see middle top panel of Fig. 4). At first glance one could be tempted to consider a resolved WDMS binary pair. Nevertheless, the SDSS spectrum (middle bottom panel of the same figure) shows the typical Balmer lines of an A star in the blue, while at redder wavelengths the typical spectral features of a low-mass star can be detected. This implies that these two systems are superimposed stars in the same image rather than being a resolved WDMS binary pair (see below).

SDSS images can also help identifying WDMS binaries among our sample that are spatially resolved in the SDSS images, but close enough that flux from both stars will enter into the spectroscopic fibre. In such cases, the SDSS magnitudes are often discrepant with the flux-calibrated SDSS spectrum, and/or have large errors as consequence of the deblending applied by the photometric pipeline. Fig. 4 (top right panel) shows the SDSS image of SDSSJ 025306.37+001329.2, which clearly reveals a spatially resolved pair of stars. The SDSS spectrum of SDSSJ 025306.37+001329.2 contains the typical signatures of a WDMS binary, i.e. broad Balmer lines from the white dwarf and TiO absorption bands from the M-dwarf, however, the errors on the SDSS magnitudes are untypically large, and do not match well the flux calibrated SDSS spectrum (bottom left panel of Fig. 4).

3. Stellar parameters

The spectroscopic data provided by the SDSS project are of sufficient quality to estimate the stellar parameters of the WDMS binaries in our catalogue. For this purpose, we have developed a procedure which decomposes the WDMS binary spectrum into its white dwarf and main

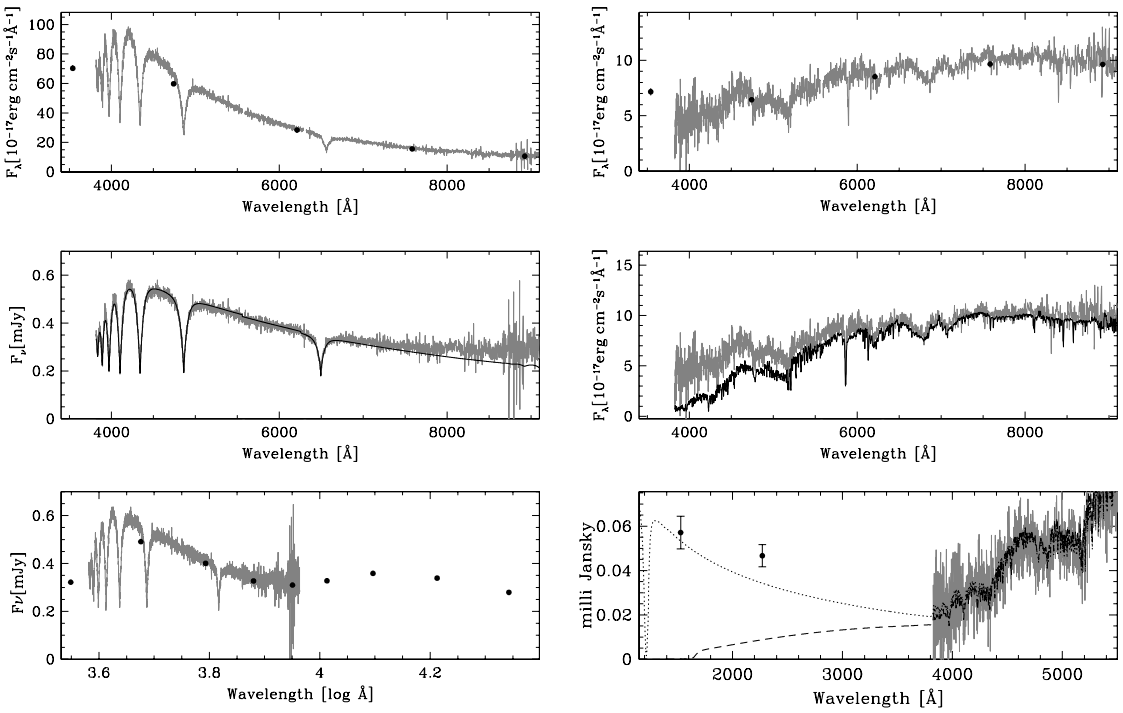

Figure 3. Top left: SDSS spectrum (gray) of SDSSJ 132925.21+123025.5, a WDMS candidate initially catalogued as single DA white dwarf. The black dots represent the SDSS magnitudes. Middle left panel: the best white dwarf model fit is superimposed in black, unambiguously identifying the red excess of the secondary star in the binary. Bottom left panel: SDSS and UKIDSS magnitudes (black dots) superimposed to the SDSS spectrum (gray). Again, the UKIDSS magnitudes clearly show the presence of a low-mass companion. Top right panel: the same for SDSSJ 131928.80+580634.2, an initially catalogued early M-type star. Middle and bottom right panels: the best M-type fit and the near- and far-ultraviolet GALEX magnitudes (black dots) clearly confirm the presence of a white dwarf primary, respectively. The dotted and dashed lines represent the white dwarf solutions (dotted for the hot, dashed for the cold) obtained from decomposing/fitting the spectrum (see Sect 3).

sequence star components, determines the spectral type of the companion by means of template fitting, and derives the white dwarf effective temperature and surface gravity from spectral model fitting (Rebassa-Mansergas et al. 2007). Assuming an empirical spectral type-radius relation for the secondary star and a mass-radius relation for the white dwarf from an updated list of Bergeron et al. (1995)'s tables, two independent distance estimates are calculated from the flux scaling factors of the template/model spectra.

In the course of decomposing/fitting the WDMS binary observations, we make use of a grid of observed M-dwarf templates, a grid of observed white dwarf templates, and a grid of white dwarf model spectra. High S/N ratio M-dwarf templates matching the spectral coverage and resolution of the WDMS binary data were produced from a few hundred late-type SDSS spectra from DR4. These spectra were classified using the M-dwarf templates of Beuermann et al. (1998). We also compiled a library of 490 high S/N DA white dwarf spectra from DR4 covering the entire observed range of $T_{\rm eff}$ and $\log g$. Finally, we computed a grid of synthetic DA white dwarf spectra using the model atmosphere code described by Koester et al. (2005), covering

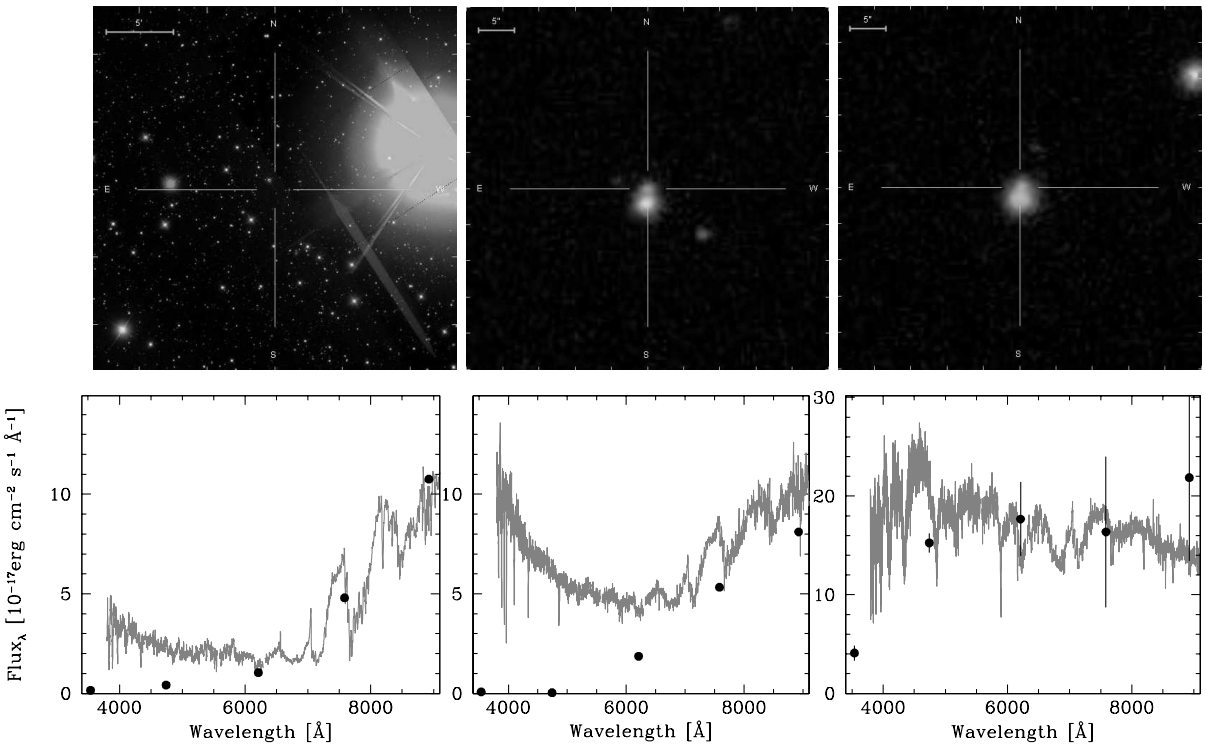

Figure 4. Top left panel: SDSS image of SDSSJ 073531.86+315015.2 (5 arcmin scale), a single red star initially considered as a WDMS binary candidate. Bottom left panel: SDSS magnitudes (black dots) and spectrum (gray) of the same system. The light from the saturated bright star (Castor A/B) is also dispersed in the spectrum. The magnitudes are consistent with those of a single red star. Top middle panel: SDSS image of SDSSJ 005827.24+005642.6 (5 arcsec scale). The image suggests a resolved WDMS binary pair. Middle bottom panel: the detection of the Balmer lines typical of an A star in the blue, together with the typical spectral features of a low-mass main sequence star in the red (gray), indicate that these are two single stars superimposed in the same image rather than a resolved WDMS binary pair. SDSS magnitudes are indicated with black dots, and are consistent with those of a low-mass star. Top right panel: SDSS image of SDSSJ 025306.37+001329.2 (5 arcsec scale), a resolved WDMS binary in our sample. Bottom right panel: SDSS magnitudes (black dots) and spectrum (gray) of the same system. Whilst the SDSS spectrum clearly shows both components, the SDSS magnitude errors are untypically large (see text for details).

$\log g = 5.0 - 9.5$ in steps of 0.25 and $T_{\rm eff} = 6000 - 100000$ K in 37 steps nearly equidistant in $\log(T_{\rm eff})$.

Our approach is a two-step procedure. In a first step, we fitted the WDMS binary spectra with a two-component model and determined the spectral type of the M-dwarf. Once the best-fit M-dwarf template has been determined and scaled appropriately in flux, it is subtracted from the WDMS binary spectrum. The residual white dwarf spectrum is then fitted with the grid of DA models described above. We then use the $T_{\rm eff}$ and $\log g$ from the fits to the whole spectrum, continuum plus lines, to select the "hot" or "cold" solution from the line profile fits (see Rebassa-Mansergas et al. 2007 for further details).

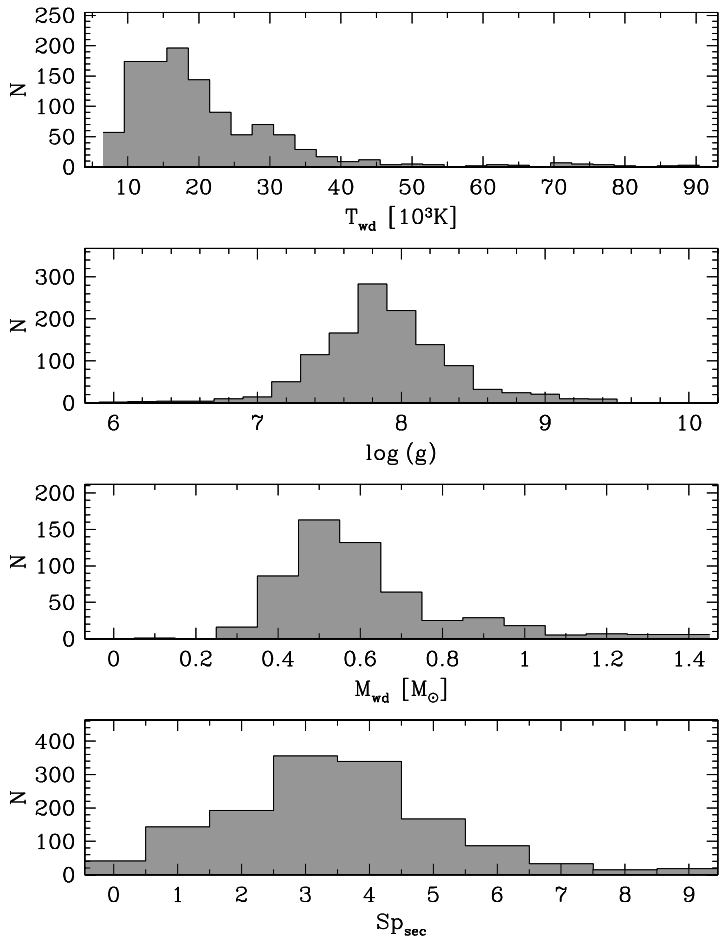

Figure 5. White dwarf $T_{\rm eff}$, $\log g$, mass, and spectral type of the secondary histograms obtained from the SDSS WDMS binaries in our catalogue. Excluded are those systems with individual white dwarf masses, $T_{\rm eff}$, and $\log g$ associated to relative errors larger than 25 per cent.

3.1. Distribution of the stellar parameters

Having determined stellar parameters for each individual system in Sect. 3, we now look at their global distribution within our sample of WDMS binaries. Figure. 5 shows histograms of the white dwarf effective temperatures, masses, $\log g$, and the spectral types of the main sequence companions. The most frequent white dwarf temperatures are between 10 000–20 000 K, white dwarf masses cluster around $M_{\rm wd} \simeq 0.5\,{\rm M}_{\odot}$, and the companion stars have most typically a spectral type M3–4, with spectral types later than M7 or earlier than M1 being very rare.

At closer inspection, the distribution of white dwarf masses has a pronounced tail towards lower masses. A tail of lower-mass white dwarfs, peaking around $0.4\,{\rm M}_{\odot}$ is observed also in well-studied samples of single white dwarfs (Liebert et al. 2005), and is interpreted as He-core white dwarfs descending from evolution in a binary star. In a sample of WDMS, a significant fraction of systems will have undergone a CE phase, and hence the fraction of He-core white dwarfs among WDMS is expected to be larger than in a sample of single white dwarfs.

The cut-off at early spectral types in the bottom panel of Fig. 5 is due to the fact that WDMS with K-type companions can only be identified from their spectra/colours if the white dwarf is very hot – and hence, very young, and correspondingly only few of such systems are in the total

SDSS WDMS sample. The cut-off seen for low-mass companions is not so trivial to interpret. Obviously, very late-type stars are dim and will be harder to be detected against a moderately hot white dwarf. Such a bias was discussed by Schreiber & Gänsicke (2003) for a sample of ~ 30 well-studied WDMS which predominantly originated from blue-colour (= hot white dwarf) surveys. However, old WDMS with cool white dwarfs should be much more common (Schreiber & Gänsicke 2003), and SDSS, sampling a much broader colour space than previous surveys, should be able to identirfy WDMS containing cool white dwarfs plus very late type companions. The relatively low frequency of such systems in the SDSS spectroscopic data base suggests that either SDSS is not efficiently targeting those systems for spectroscopic follow-up, or that they are rare in the first place, or a combination of both.

References

Adelman-McCarthy J K et al. 2008 *ApJS* **175** 297-313
Bergeron P Wesemael F and Beauchamp A 1995 *PASP* **107** 1047
Beuermann K Baraffe I Kolb U and Weichhold M 1998 *A&A* **339** 518-524
Bochanski J J West A A Hawley S L and Covey K R 2007 *AJ* **133** 531-544
Davis P J Kolb U Willems B and Gänsicke B T 2008 *MNRAS* **389** 1563-1576
de Kool M 1992 *A&A* **261** 188-202
Eisenstein D J et al. 2006 *ApJS* **167** 40-58
Iben I J and Livio 1993 *PASP* **105** 1373-1406
Koester D Napiwotzki R Voss B Homeier D and Reimers D 2005 *A&A* **439** 317-321
Liebert J Bergeron P and Holberg J B 2005 *ApJS* **156** 47-68
Nebot Gomez-Moran A et al. 2008, submitted
Politano M and Weiler K P 2007 *ApJ* **665** 663-679
Pyrzas S et al. 2008 submitted
Rebassa-Mansergas A Gänsicke B T Rodríguez-Gil P Schreiber M R and Koester D 2007 *MNRAS* **382** 1377-1393
Rebassa-Mansergas A et al. 2008 *MNRAS* **390** 1635-1646
Schreiber M R and Gänsicke B T 2003 *A&A* **375** 937
Schreiber M R Nebot Gomez-Moran A and Schwope A D 2007 *Astronomical Society of the Pacific* **372** 459
Schreiber M Gänsicke B T Southworth J Schwope A D and Koester D 2008 *A&A* **484** 441-450
Silvestri M N et al. 2007 *AJ* **134** 741-748
Stoughton C et al. 2002 *AJ* **123** 485-548
Webbink R F 19884 *ApJ* **277** 355-360
Webbink R F 2007 *Preprint* ArXiv e-prints/0704.0280
Willems B and Kolb U 2004 *A&A* **419** 1057-1076
York D G et al. 2000 *AJ* **120** 1579-1587